RESEARCH ARTICLE | MAY 30 2023

An improved synthetic signal injection routine for the Haloscope At Yale Sensitive To Axion Cold dark matter (HAYSTAC)

Yuqi Zhu ; M. J. Jewell ; Claire Laffan; Xiran Bai ; Sumita Ghosh ; Eleanor Graham ; S. B. Cahn; Reina H. Maruyama ; S. K. Lamoreaux

Rev Sci Instrum 94, 054712 (2023)
https://doi.org/10.1063/5.0137870

Review of Scientific Instruments | ARTICLE | scitation.org/journal/rsi

An improved synthetic signal injection routine for the Haloscope At Yale Sensitive To Axion Cold dark matter (HAYSTAC)

Cite as: Rev. Sci. Instrum. 94, 054712 (2023); doi: 10.1063/5.0137870
Submitted: 6 December 2022 • Accepted: 12 May 2023 •
Published Online: 30 May 2023

Yuqi Zhu,[1,2,a)] M. J. Jewell,[1,2] Claire Laffan,[1,2] Xiran Bai,[1,2] Sumita Ghosh,[2,3] Eleanor Graham,[1,2] S. B. Cahn,[1,2] Reina H. Maruyama,[1,2,b)] and S. K. Lamoreaux[1,2]

AFFILIATIONS

[1] Department of Physics, Yale University, New Haven, Connecticut 06520, USA
[2] Wright Laboratory, Department of Physics, Yale University, New Haven, Connecticut 06520, USA
[3] Department of Applied Physics, Yale University, New Haven, Connecticut 06520, USA

[a)] **Present address:** Stanford University, Stanford, CA 94305, USA.
[b)] **Author to whom correspondence should be addressed:** reina.maruyama@yale.edu

ABSTRACT

Microwave cavity haloscopes are among the most sensitive direct detection experiments searching for dark matter axions via their coupling to photons. When the power of the expected microwave signal due to axion–photon conversion is on the order of 10^{-24} W, having the ability to validate the detector response and analysis procedure by injecting realistic synthetic axion signals becomes helpful. Here, we present a method based on frequency hopping spread spectrum for synthesizing axion signals in a microwave cavity haloscope experiment. It allows us to generate a narrow and asymmetric shape in frequency space that mimics an axion's spectral distribution, which is derived from a Maxwell–Boltzmann distribution. In addition, we show that the synthetic axion's power can be calibrated with reference to the system noise. Compared to the synthetic axion injection in the Haloscope At Yale Sensitive to Axion Cold dark matter (HAYSTAC) Phase I, we demonstrated synthetic signal injection with a more realistic line shape and calibrated power.

I. INTRODUCTION

The axion is a well-motivated solution to the strong charge-parity problem in quantum chromodynamics and is also a dark matter candidate.[1–4] The most sensitive direct detection experiments by far are based on the microwave cavity haloscope technique.[5] In a haloscope experiment, the axions would convert into photons of equal energy inside a resonant microwave cavity permeated by a strong magnetic field. The energy of each axion-converted photon would be equal to the axion's total energy—the sum of its rest-mass energy m_a and kinetic energy. Therefore, the line shape of the resulting microwave signal appearing in a haloscope experiment would inherit the axion's kinetic energy distribution. Suppose that $\nu_a = m_a/(2\pi)$ is the axion mass in SI-frequency units, and we denote the spectral distribution of an axion with mass m_a as $f_{\nu_a}(\nu)$. The distribution $f_{\nu_a}(\nu)$ encodes the axion's properties derived from the pseudo-isothermal halo model[6] and accounts for the modulation due to the Earth's rotation around the center of the galaxy.[7,8] Here, we describe a method to synthesize a microwave signal whose line shape resembles that of an expected axion signal. Injecting and detecting such synthesized signals into the detector allows us to characterize the detector's response, validate the analysis procedure,[8–10] and perform a blind analysis.[11]

Our method for synthesizing axion signals is inspired by a patent for radio frequency (rf) hopping by Markey and Antheil;[12] it is related to the frequency hopping spread spectrum (FHSS) technique, which has been applied in military and wireless communication to prevent interception and reduce interference. In our experiment, this technique allows us to generate an axion's spectrum by hopping between a large number of random rf tones sampled from the axion's spectral distribution. This way, we can produce the spectral spread associated with the axion's kinetic energy distribution. As will become more apparent later, the axion's line shape function is asymmetric and narrow. The frequency hopping method allows us to overcome the technical difficulties associated with signal shaping in the frequency domain. In principle, this technique can be used to synthesize any generic spectral shapes. It is also a realistic simulation: each axion's energy is a random variable that follows $f_{\nu_a}(\nu)$ and the observed line shape is an ensemble-averaged result.

In this article, we describe the methods involved in signal injection in Sec. II and provide a summary and outlook in Sec. III.

II. METHODS

The synthetic axion signal is injected as a transmission (tx) input through the weak port of the cavity and subsequently coupled out from the receiver's port. Figure 1 shows the schematic of synthetic signal injection. The main device that synthesizes axion signals is an analog signal generator (model: Agilent E8257D), labeled PSG2. In between PSG2 and the cavity's weak port, an rf switch (model: ZFSWA2-63DR+) and a power splitter/combiner (model: ZX10-2-71-S+) are added in this order. The rf switch allows us to interrupt signal injection from PC1 via a USB DAC (model: USB-6009-NI). For instance, the injection signals are blocked during calibration measurements between axion datasets, as they would bias the noise measurement. The power splitter allows us to simultaneously send in a weak tone near the JPA resonance as a way to monitor and stabilize the JPA gain.[9] The variable temperature stage (VTS) allows us to carry out *in situ* noise calibration[8] as part of the power calibration for the axion signal injected. The Haloscope At Yale Sensitive To Axion Cold dark matter (HAYSTAC) has been using squeezed-state receivers since 2021.[13,14] The squeezing JPA (SQZ) is also included in this diagram, as it affects the total noise, even though the injected signal does not go through it. The full scheme with additional details for the squeezed-state receiver chain can be found in Refs. 13–15.

To synthesize the microwave signal for injection, we use the "Step (digital) sweep" mode of PSG2 by providing it with a list of frequencies, amplitudes, and dwell times. In aggregate, the list of rf tones would reproduce the axion's line shape. In this experiment, by default, we fix the amplitude and dwell time and only change the frequency of each point. The frequency precision is set to 0.1 kHz, or 8 significant digits for a GHz frequency, chosen based on the precision of data acquisition. Due to the device's output-byte limit during transmission, the maximum length for such a list is about $n_8 = 35$. For sub-kHz frequency precision, we empirically found that $N \gg 2000$ samples are needed to reveal the shape of the sampling distribution. Therefore, to iterate through a list with $N \gg n_8$ rf tones, it is necessary to transmit $\lceil N/n_8 \rceil$ sublists. To begin, we establish the connection between PSG2 and PC2 via virtual instrument software architecture (VISA) and enable the rf output on PSG2. The steps for sending N rf tones are as follows:

1. Send n_8 frequencies, dwell time τ_d, and amplitude P_{syn} to PSG2 from PC2 in one command.
2. Wait for τ_w before sending another command to PSG2. Here, $\tau_w = n_8\tau_d + \tau_r$ includes the time required for the sweep $n_8\tau_d$ and an additional uniformly random delay between 2 and 5 s $\tau_r \sim U(2, 5)$ required for VISA communication.

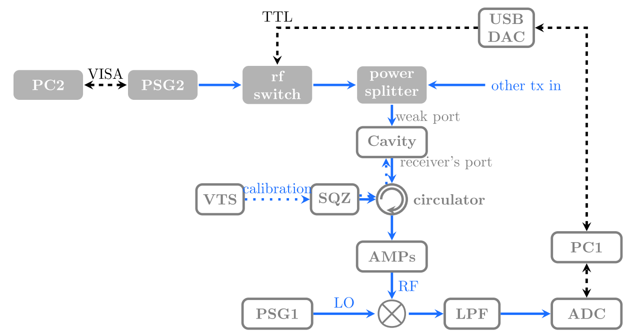

FIG. 1. Schematic. The new components added for hardware injection are shown as gray nodes; the rest already exist as part of the experiment. The blue arrows and black dashed arrows indicate analog and digital signals, respectively. PC2 controls PSG2 to inject a number of rf tones whose frequencies are sampled from $f_{\nu_a}(\nu)$ to simulate axions with mass ν_a. The synthetic axion signals are injected through the weak port of the cavity and then measured and amplified by the receiver chain consisting of two amplifiers (AMPs): a JPA followed by a high-electron-mobility transistor. Subsequently, the amplified signals are down-converted, mixed with the local oscillator (LO) signal provided by PSG1, and then filtered by the low-pass filter (LPF). The time-series signal collected by the Analog/Digital Converter (ADC) is then Fourier transformed into an intermediate-frequency (IF) spectrum. The VTS helps us characterize the system's total noise by comparing the cavity's spectrum to blackbody spectra at controlled temperatures. The signal from the VTS is only coupled in during a calibration measurement, as indicated by the dotted blue arrows.

3. Check PSG2's status to confirm that the sweep has been completed. If not, generate an error message reporting PSG2's status (settling or sweeping) and wait 2 more seconds before checking the status again.
4. Repeat steps 1–3 until all N items are iterated over.

Based on the timing parameters, we can derive the average duty cycle of this signal injection routine as $\bar{\eta} = n_8\tau_d/\bar{\tau}_w$, after averaging over $\lceil N/n_8 \rceil \gg 1$ repetitions. By default, the dwell time is $\tau_d = 5$ ms, resulting in $\eta = 4.8\% \pm \frac{1\%}{\lceil N/n_8 \rceil}$. In step 2, τ_r is randomized to avoid introducing any additional frequency patterns into the signal.

A. Rejection sampling

To generate a list of random frequencies for signal injection, the probability density function of the sampling distribution is the axion's spectral function,

$$f_{\nu_a}(\nu) = \frac{2}{\sqrt{\pi}}\left(\sqrt{\frac{3}{2}}\frac{1}{r}\frac{1}{\nu_a\langle\beta^2\rangle}\right)\sinh\left(3r\sqrt{\frac{2(\nu-\nu_a)}{\nu_a\langle\beta^2\rangle}}\right) \times e^{-\frac{3(\nu-\nu_a)}{\nu_a\langle\beta^2\rangle}-3r^2/2}, \tag{1}$$

where $\sqrt{\langle v^2\rangle} \approx 270$ km/s is the virial velocity, $\langle\beta^2\rangle = \langle v^2\rangle/c^2 \approx 8 \times 10^{-7}$ (c is the speed of light), $v_s \approx 220$ km/s is the orbital velocity of the solar system about the center of the galaxy, and $r = v_s/\sqrt{\langle v^2\rangle} \approx \sqrt{2/3}$.[8] Given the function form of f_{ν_a}, it can be seen that applying inverse transform sampling to sample from it is not obviously trivial. Here, we use rejection sampling[16] as an alternative. To apply it, we find another distribution whose probability density function $y(\nu)$

satisfies $\xi \cdot y(\nu) > f_{\nu_a}(\nu)\ \forall \nu$ for some $\xi > 0$. In our case, the Cauchy distribution

$$y(\nu) = \frac{1}{\sigma\pi} \frac{1}{1 + ((\nu - \mu)/\sigma)^2}, \tag{2}$$

with $\mu = \nu_a + 1$ kHz and $\sigma = 3$ kHz, is sufficient because as $\nu \to \infty$, $f_{\nu_a}/y \to 0$. Furthermore, the cumulative function of a Cauchy distribution is invertible; therefore, it is straightforward to apply inverse transform sampling to a sample from y. Let us consider rejection sampling as an iterative process. In each iteration, we sample a random number from y, noting it as ν', and then decide whether to reject or accept it based on another random number, u, chosen from the uniform random distribution between 0 and 1. If $u \le f_{\nu_a}(\nu')/(\xi \cdot y(\nu'))$, we accept ν'; otherwise, reject it. This iteration continues until we have N samples. Figure 2 shows the outcome of this method when the sampling distribution is f_{ν_a} with $\nu_a = 4.721\,630\,0$ GHz as an example. It can be seen that the overall acceptance rate depends on the ratio of $\int d\nu f_{\nu_a}$ to $\int d\nu \xi \cdot y$, i.e., the ratio of areas under f_{ν_a} and $\xi \cdot y$; with $\xi = 3$, $\int d\nu f_{\nu_a} / \int d\nu\, \xi \cdot y \approx 0.3$.

B. Validation of spectral shape

The validation of this procedure is performed with an ~10 h signal injection run to verify that the signal has the correct spectral shape. The injection is done at a relatively high power such that the signal is clearly visible above the noise even without the standard processing.[8] This decouples any deviations caused by the injection routine from the shape changes introduced by the processing and filtering scheme used to analyze the data. The observed signal is fit to the expected shape given by Eq. (1) in a 30 kHz window around the injected frequency. The fit model includes a linear background component to approximately capture the spectral shape of the cavity in this range. The results from the fit in which only the amplitude of the expected signal per Eq. (1) and the background model parameters are floating are shown in Fig. 3. This results in a χ^2/ndf of 1.57, showing good agreement between the observed and injected signal shapes. The χ^2/ndf can be improved minimally to 1.56 when allowing the width of the line shape to float by also varying the virial velocity, but remains within 1% of the true velocity used in the injection.

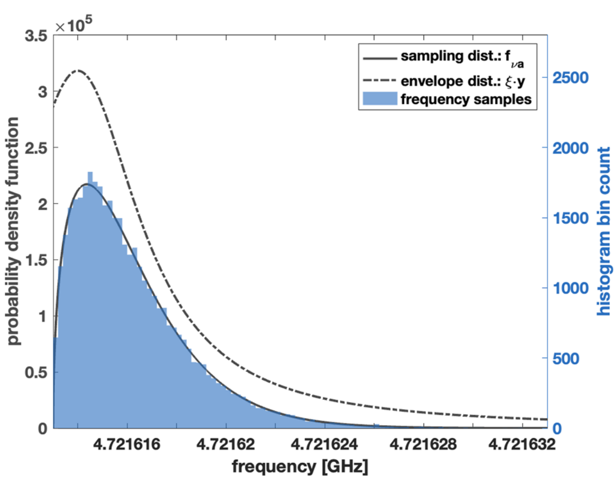

FIG. 2. Applying rejection sampling to create a list of $N = 40\,000$ random frequencies from an axion's spectral distribution with $\nu_a = 4.721\,630\,0$ GHz. The envelope distribution (dashed–dotted gray line) for the sampling distribution f_{ν_a} (solid gray line) is obtained by scaling the Cauchy distribution y by $\xi = 3$. The histogram (blue) shows that the samples obtained using this method conform to the sampling distribution f_{ν_a}.

C. Power calibration

Although the power of each rf tone injected can be programmed on PSG2, neither the weak port's coupling efficiency nor the transmission line loss is known, so it is necessary to carry out a power calibration measurement to determine the time-averaged power of a synthetic axion signal. At a fixed cavity frequency, suppose that we inject axions, each with power P_{syn}, near the cavity resonance for duration τ_{int}. The observed signal-to-noise ratio (SNR) depends on the system noise power at the injected axion's detuning with respect to the cavity frequency ν_c, $h\nu_c N_{sys}(|\nu_a - \nu_c|)$ (h is the Planck constant), P_{syn}, τ_{int}, η, and the measurement bandwidth, which is chosen to match the axion linewidth $\Delta\nu_a \sim \nu_a/10^6$. This then allows us to estimate P_{syn} from a standard axion measurement,

$$P_{syn} = \text{SNR} \cdot (h\nu_c N_{sys}(|\nu_a - \nu_c|)) \cdot \sqrt{\frac{\Delta\nu_a}{\eta\tau_{int}}}. \tag{3}$$

As an example, Fig. 4 shows some results from a 12-h measurement with the cavity and JPA at fixed frequencies. These data are taken at a lower injected power to produce a more realistic signal that is closer to the detection threshold of the experiment. From this dataset, SNR and N_{sys} are derived following the analysis routine outlined in Ref. 8. Each raw spectrum is first normalized by dividing out the average baseline. This step allows us to identify bins contaminated by IF noise. After removing contaminated bins from the first normalized spectrum, the spectrum is normalized again by dividing out the Savitzky–Golay fit to itself and subtracting 1. Then, the resulting

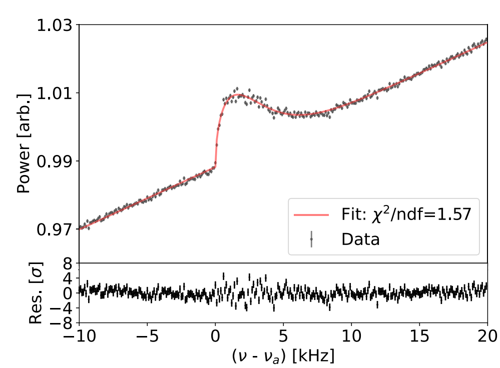

FIG. 3. (Top) The observed power in a 30 kHz window near an injected signal from a high power injection run. To validate the signal shape, the spectrum is minimally processed with no filtering applied. A fit to the line shape in Eq. (1) is shown as a solid line. This fit includes a linear $(m\nu + b)$ background component to capture the cavity's spectral variation over this range. The residuals between the fit and data are shown in the bottom panel and give a χ^2/ndf = 1.57, showing good agreement between the observed and injected spectral shapes.

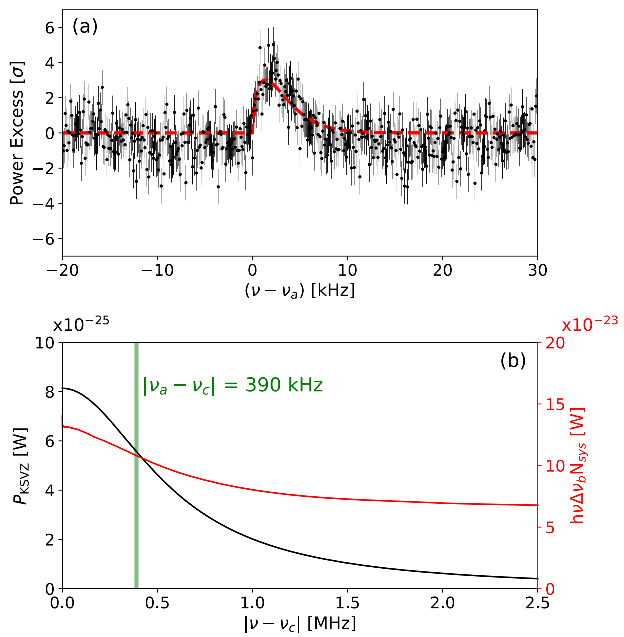

FIG. 4. (a) Power excess (points) in the combined spectrum normalized to the expected standard deviation (error bars) and overlaid with f_{ν_a} (dashed line) in a 50 kHz window around the synthetic axion signal. (b) Expected signal power P_{KSVZ} (black) and system noise $h\nu_c N_{\mathrm{sys}}$ integrated over an analysis bin width $\Delta\nu_b$ (red) at a fixed cavity frequency ν_c as functions of detuning $|\nu - \nu_c|$. The green shaded region indicates the frequencies within $\Delta\nu_a$ of the injected signal. The cavity presents a noise source to the receiver that is frequency dependent with ~1.1 MHz bandwidth and varies with $|\nu - \nu_c|$. The response to an axion signal has a different frequency dependence that is more sharply peaked at the cavity resonance. The plot shows the detuning-dependent variation of the axion signal and system noise.

spectrum are rescaled to account for the detuning-dependent sensitivity and summed to produce a combined spectrum. This spectrum is normalized to the expected standard deviation in each bin, as shown in Fig. 4(a). To derive the SNR of the injected signal, we find the total power of the injected signal by convolving the spectrum in Fig. 4(a) with the axion line shape function f_{ν_a}. In this case, the resulting SNR is about 17.6. The scale factor used in producing the rescaled spectrum is the ratio between the noise power per analysis bin $\Delta\nu_b = 100$ Hz and the expected signal power, both of which are plotted in Fig. 4(b). At detuning $|\nu_a - \nu_c| \sim 390$ kHz, the power of an axion-converted microwave signal is expected to be $P_{\mathrm{KSVZ}} = 5.6(1) \times 10^{-25}$ W, assuming the axion–photon coupling strength $g_{a\gamma\gamma}$ (appearing in the axion–photon Lagrangian) in the Kim–Shifman–Vainshtein–Zakharov (KSVZ) model[17,18] $g_{a\gamma\gamma}^{\mathrm{KSVZ}} = (-3.70 \times 10^{-7}/\mathrm{MeV}^2) \cdot m_a$ nominally.[9] This is calculated from various experimental parameters, including the magnetic field strength and cavity volume.[13,19] The system noise in units of photon numbers, $N_{\mathrm{sys}}(|\nu_a - \nu_c|) = 0.26(2)$, is derived from *in situ* calibration measurements.[13–15] Evaluating Eq. (3) with these values, we find $P_{\mathrm{syn}} = 2.2(2) \times 10^{-23}$ W, and that the injected axions have a coupling strength at $6.2(5)\, g_{a\gamma\gamma}^{\mathrm{KSVZ}}$ level.

III. SUMMARY

We demonstrated synthetic axion injection using the rf hopping method.[20] The injected axion has the spectral distribution of a cold dark matter axion, and its power is calibrated using the total noise power as a reference. This is a more realistic synthetic signal, in terms of spectral shape and power, as compared to the prior demonstration in HAYSTAC Phase I (cf. Appendix F in Ref. 8). Furthermore, as HAYSTAC and other axion haloscope experiments, including CAPP and ADMX, enter the data production phase, mitigating bias will become increasingly important.[21] For instance, salting and blinding have become integral parts of WIMP (weakly interacting massive particle) dark matter searches.[22,23] The method we developed can serve as the basis for implementing blinding and salting for axion dark matter searches.

ACKNOWLEDGMENTS

We acknowledge the full HAYSTAC collaboration for the apparatus we used in this experiment, including the microwave cavity and JPAs. Y.Z. thanks Joseph Howlett for the helpful discussion and references on mitigating bias in dark matter searches. HAYSTAC is supported by the National Science Foundation under Grant Nos. PHY-1701396, PHY-1607223, PHY-1734006, and PHY-1914199 and by the Heising-Simons Foundation under Grant Nos. 2014-0904 and 2016-044. Y.Z., S.G., E.G., S.B.C., M.J.J., and R.H.M. were supported in part by the Department of Energy under Grant No. DE-AC02-07CH11359. S.B.G. was supported in part by the National Science Foundation under Grant No. DMR-1747426.

AUTHOR DECLARATIONS

Conflict of Interest

The authors have no conflicts to disclose.

Author Contributions

Yuqi Zhu: Data curation (equal); Formal analysis (equal); Investigation (equal); Writing – original draft (equal). **M. J. Jewell**: Data curation (equal); Formal analysis (equal); Investigation (equal); Writing – review & editing (equal). **Claire Laffan**: Data curation (equal); Formal analysis (equal). **Xiran Bai**: Writing – review & editing (equal). **Sumita Ghosh**: Writing – review & editing (equal). **Eleanor Graham**: Writing – review & editing (equal). **S. B. Cahn**: Writing – review & editing (equal). **Reina H. Maruyama**: Funding acquisition (equal); Project administration (equal); Writing – review & editing (equal). **S. K. Lamoreaux**: Conceptualization (lead); Funding acquisition (equal); Project administration (equal); Writing – review & editing (equal).

DATA AVAILABILITY

The data that support the findings of this study are available from the corresponding author upon reasonable request.

REFERENCES

[1] R. D. Peccei and H. R. Quinn, "CP conservation in the presence of pseudoparticles," Phys. Rev. Lett. **38**, 1440–1443 (1977).
[2] R. D. Peccei and H. R. Quinn, "Constraints imposed by CP conservation in the presence of pseudoparticles," Phys. Rev. D **16**, 1791–1797 (1977).
[3] S. Weinberg, "A new light boson?," Phys. Rev. Lett. **40**, 223–226 (1978).
[4] F. Wilczek, "Problem of strong *P* and *T* invariance in the presence of instantons," Phys. Rev. Lett. **40**, 279–282 (1978).
[5] P. Sikivie, "Experimental tests of the 'invisible' axion," Phys. Rev. Lett. **51**, 1415–1417 (1983).
[6] R. Jimenez, L. Verde, and S. P. Oh, "Dark halo properties from rotation curves," Mon. Not. R. Astron. Soc. **339**, 243–259 (2003).
[7] M. S. Turner, "Periodic signatures for the detection of cosmic axions," Phys. Rev. D **42**, 3572–3575 (1990).
[8] B. M. Brubaker, L. Zhong, S. K. Lamoreaux, K. W. Lehnert, and K. A. van Bibber, "HAYSTAC axion search analysis procedure," Phys. Rev. D **96**, 123008 (2017).
[9] B. M. Brubaker, L. Zhong, Y. V. Gurevich, S. B. Cahn, S. K. Lamoreaux, M. Simanovskaia, J. R. Root, S. M. Lewis, S. Al Kenany, K. M. Backes *et al.*, "First results from a microwave cavity axion search at 24 μeV," Phys. Rev. Lett. **118**, 061302 (2017).
[10] S. Al Kenany, M. A. Anil, K. M. Backes, B. M. Brubaker, S. B. Cahn, G. Carosi, Y. V. Gurevich, W. F. Kindel, S. K. Lamoreaux, K. W. Lehnert *et al.*, "Design and operational experience of a microwave cavity axion detector for the 20–100 μeV range," Nucl. Instrum. Methods Phys. Res., Sect. A **854**, 11–24 (2017).
[11] C. Bartram, T. Braine, E. Burns, R. Cervantes, N. Crisosto, N. Du, H. Korandla, G. Leum, P. Mohapatra, T. Nitta, ADMX Collaboration *et al.*, "Search for 'invisible' axion dark matter in the 3.3–4.2 μeV mass range," Phys. Rev. Lett. **127**, 261803 (2021).
[12] H. K. Markey and G. Antheil, "Secret communication system," U.S. Patent No. 2292387A (June 1941).
[13] K. M. Backes, D. A. Palken, S. A. Kenany, B. M. Brubaker, S. B. Cahn, A. Droster, G. C. Hilton, S. Ghosh, H. Jackson, S. K. Lamoreaux *et al.*, "A quantum enhanced search for dark matter axions," Nature **590**, 238–242 (2021).
[14] M. J. Jewell, A. F. Leder, K. M. Backes, X. Bai, K. van Bibber, B. M. Brubaker, S. B. Cahn, A. Droster, M. H. Esmat *et al.*, "New results from HAYSTAC's phase II operation with a squeezed state receiver," Phys. Rev. D **107**, 072007 (2023).
[15] K. M. Backes, "A quantum-enhanced search for dark matter axions," Ph.D. thesis, Yale University, 2021.
[16] B. D. Flury, "Acceptance–rejection sampling made easy," SIAM Rev. **32**, 474–476 (1990).
[17] M. Dine, W. Fischler, and M. Srednicki, "A simple solution to the strong CP problem with a harmless axion," Phys. Lett. B **104**, 199–202 (1981).
[18] J. E. Kim, "Weak-interaction singlet and strong CP invariance," Phys. Rev. Lett. **43**, 103–107 (1979).
[19] P. Sikivie, "Detection rates for "invisible"-axion searches," Phys. Rev. D **32**, 2988–2991 (1985).
[20] The code for implementing synthetic axion injection is made available as an open-source project at https://github.com/yuqizhuyqz/syntheticaxioninjection.git.
[21] D. Baxter, I. M. Bloch, E. Bodnia, X. Chen, J. Conrad, P. Di Gangi, J. E. Y. Dobson, D. Durnford, S. J. Haselschwardt, A. Kaboth *et al.*, "Recommended conventions for reporting results from direct dark matter searches," Eur. Phys. J. C **81** (2021).
[22] D. S. Akerib, S. Alsum, H. M. Araújo, X. Bai, A. J. Bailey, J. Balajthy, P. Beltrame, E. P. Bernard, A. Bernstein, Biesiadzinski, LUX Collaboration *et al.*, "Results from a search for dark matter in the complete LUX exposure," Phys. Rev. Lett. **118**, 021303 (2017).
[23] E. Aprile, J. Aalbers, F. Agostini, M. Alfonsi, L. Althueser, F. D. Amaro, M. Anthony, F. Arneodo, L. Baudis, B. Bauermeister, XENON Collaboration *et al.*, "Dark matter search results from a one ton-year exposure of XENON1T," Phys. Rev. Lett. **121**, 111302 (2018).